

## PRODUCTION CHARACTERISTICS OF THE F MESON

DASP Collaboration

R. BRANDELIK, W. BRAUNSCHWEIG, H.-U. MARTYN, H.G. SANDER, D. SCHMITZ,  
W. STURM<sup>1</sup> and W. WALLRAFF

*I. Physikalisches Institut der RWTH Aachen, Fed. Rep. Germany*

D. CORDS, R. FELST, R. FRIES, E. GADERMANN, H. HULTSCHIG, P. JOOS, W. KOCH,  
U. KOTZ, H. KREHBIEL, D. KREINICK<sup>2</sup>, H.L. LYNCH, W.A. McNEELY<sup>3</sup>, G. MIKENBERG<sup>5</sup>,  
K.C. MOFFEIT<sup>4</sup>, D. NOTZ, M. SCHLIWA, A. SHAPIRA<sup>5</sup>, B.H. WIJK and G. WOLF

*Deutsches Elektronen-Synchrotron DESY, Hamburg, Fed. Rep. Germany*

J. LUDWIG<sup>6</sup>, K.H. MESS<sup>7</sup>, A. PETERSEN, G. POELZ, J. RINGEL, O. ROMER, R. RÜSCH,  
K. SAUERBERG and P. SCHMÜSER

*II Institut für Experimentalphysik der Universität Hamburg, Fed. Rep. Germany*

W. de BOER, G. BUSCHHORN, W. FUES, Ch. von GAGERN, G. GRINDHAMMER,  
B. GUNDERSON, R. KOTTHAUS, H. LIERL<sup>8</sup> and H. OBERLACK

*Max-Planck-Institut für Physik und Astrophysik, München, Fed. Rep. Germany*

S. ORITO, T. SUDA, Y. TOTSUKA and S. YAMADA

*Lab. of Int. Coll. on Elementary Particle Physics and Department of Physics, University of Tokyo, Japan*

Received 6 November 1978

Inclusive cross sections of  $\eta$  production by  $e^+e^-$  annihilation for c.m. energies between 4.0 and 5.0 GeV are presented. The  $\eta$  production is shown to be correlated with the production of a weakly decaying particle, indicating that its main source is F production. At the 4.42 GeV resonance it is correlated with a low energy photon, suggesting  $F\bar{F}^*$  or  $F^*\bar{F}$  production. A mass determination of the F is made at 4.42 GeV using the  $F \rightarrow \eta\pi$  decay channel.

**1. Introduction.** In a previous publication of this collaboration [1], the first evidence for the production of the F meson and the existence of the  $\eta\pi$  decay mode were presented. Since then more data have been

<sup>1</sup> Now at Beiersdorf A.G., Hamburg.

<sup>2</sup> Now at Cornell University.

<sup>3</sup> Now at Boeing Computer Services, Seattle, Washington.

<sup>4</sup> Now at SLAC.

<sup>5</sup> On leave from the Weizmann Institute, Rehovot, Israel.

<sup>6</sup> Now at California Institute of Technology.

<sup>7</sup> Now at CERN.

<sup>8</sup> Now at University of Dortmund.

accumulated at various c.m. energies, in particular at 4.4 GeV. In this paper results are presented based on all data using improved energy resolution obtained in the case of spatially overlapping photon showers. Also, quantitative results are given for the total inclusive  $\eta$  cross section, and an attempt is made to determine, in a model dependent way, the total F production cross section.

**2. Data.** Data were collected at the  $e^+e^-$  storage ring DORIS for c.m. energies between 3.99 and 5.0

GeV using the DASP detector [2]. For the purpose of analysis, the data have been grouped into five regions, 3.99 to 4.10 = "4.03" GeV ( $1178 \text{ nb}^{-1}$ ), 4.10 to 4.23 = "4.17" GeV ( $509 \text{ nb}^{-1}$ ), 4.23 to 4.36 = "4.30" GeV ( $603 \text{ nb}^{-1}$ ), 4.36 to 4.49 = "4.42" GeV ( $2240 \text{ nb}^{-1}$ ), 4.5 to 4.99 = "4.60" GeV ( $727 \text{ nb}^{-1}$ ) and 4.99 to 5.01 = "5.0" GeV ( $1270 \text{ nb}^{-1}$ ). The numbers in quotes are the average energies weighted by the luminosity for a given interval, and those in parentheses are integrated luminosities for each data set.

The DASP detector has been discussed elsewhere [2]; for the purpose of this analysis the inner detector was mainly used, which consists of various layers of proportional chambers, proportional tubes, and lead-scintillator sandwich counters, which measure the direction of the charged particles as well as the direction and the energy of the photons. The detection efficiency for photons was 50% at 0.05 GeV, rising to 80% at 0.1 GeV and 95% above 0.3 GeV. The measured energy resolution of the combined shower and scintillation counters is  $\sigma(E) = 0.14\sqrt{E(\text{GeV})}$  for  $E > 0.05$  GeV. The angular resolution for photons in both the polar angle ( $\theta_\gamma$ ) with respect to the  $e^+$  direction and azimuthal ( $\phi_\gamma$ ) angle, is 0.03 radians.

The data analysis procedure consisted of two levels. At the first level, events were selected by a computer program. These events were then scanned by a physicist to check the photon identification, and in particular to resolve ambiguities and improve the energy determination in the case of overlapping tracks<sup>†1</sup>. The computer selection required that there are at least two but not more than six charge tracks, and at least two but not more than six photons. Photons with energies between 0.14 and 1.0 GeV have been considered candidates in the determination of the two photon mass spectrum  $M(\gamma_i, \gamma_j)$ . The vector sum of the momentum of the two photons ( $\gamma_i, \gamma_j$ ) has been required to be between 0.3 and 1.4 GeV, and the angle between them to be larger than  $11.5^\circ$ . For the purpose of reducing

background, it has also been required that at least 0.1 GeV be deposited in both forward and backward hemispheres with respect to the  $e^+$  direction. In the scanning stage, the following cuts were imposed on photons to be included in the  $M(\gamma_i, \gamma_j)$  plot. a) They should not be in a DASP half octant containing two or more tracks in addition to that photon. b) They should not share a shower counter with a charged track, and c) the photon shower should be well separated from a nearby track (5 cm in space) in at least one  $30^\circ$  view of the proportional tubes. In the case of two photons overlapping in either the scintillator or in the shower counters, the total energy deposited in these counters was subdivided amongst the two photons according to the number of sparks observed in the proportional tube counter. This results in an energy resolution of  $\sigma \approx 0.3\sqrt{E(\text{GeV})}$  for overlapping photons.

Due to a malfunction of one of the scintillators, the data at 4.03 GeV have been subjected to the additional requirement  $|\phi_\gamma| < 2.51$ ; this implies a reduction in acceptance by 25%.

Events containing a photon of less than 0.14 GeV are called "low energy photon events".

**3. Results.** Fig. 1 shows the two-photon effective mass distribution for the various center of mass energies; while a clear  $\pi^0$  peak is seen at all energies,  $\eta$  signals are clearly seen only at 4.17 and 4.42 GeV, and possibly at 4.60 GeV. The lack of an  $\eta$  signal at the 4.03 GeV resonance, which is dominated by  $DD^*$  and  $D^*\bar{D}^*$  production, indicates that the branching ratio for the decay  $D \rightarrow \eta + \text{anything}$  is small.

The number of  $\eta$ 's observed at each energy has been determined by two methods.

**Method I:** In order to separate the background due to wrong photon pairing from the genuine  $\eta$  and  $\pi^0$  signal in the  $\gamma\gamma$  invariant mass spectrum, photons from two different events with equal number of photons were combined to produce the effective masses  $M(\gamma_{\text{event 1}}, \gamma_{\text{event 2}})$ . The resulting distribution was assumed to describe the shape of the background and was used together with the  $\eta$  and  $\pi^0$  shapes to fit the observed  $M(\gamma\gamma)$  distribution in the various energy intervals investigated. The results of these fits are given as solid lines in fig. 1. The distributions at 4.03, 4.30 and 5 GeV required negative amounts of  $\eta$ 's, and therefore the fitted curves correspond to a sum of  $\pi^0$  and background only.

<sup>†1</sup> The DASP detector is subdivided into 8 independent geometrical modules. Two of these form the front end of the outer magnetic spectrometers, and are not used for the inner detector photon analysis. The remaining 6 octants are subdivided each into two geometrically independent 1/2 octants by a plane perpendicular to the  $e^+e^-$  axis. The fiducial volume cut for photons is given by  $|\cos \theta_\gamma| < 0.8$ ,  $0.41 \leq |\phi_\gamma| < 2.73$  while the region  $0.15 \leq \|\phi_\gamma\| - \pi/2 \leq 0.54$  is excluded.

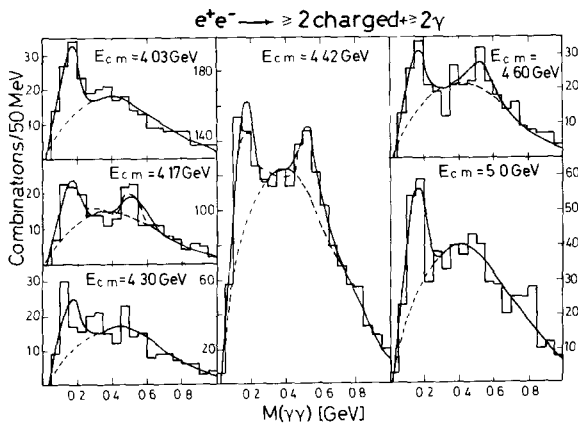


Fig. 1  $M(\gamma\gamma)$  mass distribution at the various c.m. energies. The solid lines are the results of a fit to a sum of background,  $\pi^0$  and  $\eta$  contributions. The dashed lines correspond to the amount of background required by the fit under the  $\eta$  and  $\pi^0$  peaks. The dashed-dotted lines at 4.17 and 4.42 GeV are the results of a fit corresponding to the sum of F production and the background, described by the  $M(\gamma\gamma)$  mass distribution at  $E_{c.m.} = 4.03$  GeV.

Method II: Here the shapes of two distributions arising from different physics sources were fitted to the observed  $M(\gamma\gamma)$  spectrum. The first contribution comes from normal u, d, s physics and from D production which were assumed to be sufficiently well described by the shape of the  $M(\gamma\gamma)$  spectrum observed in the 4.03 GeV energy interval. The second contribution is due to F production which was assumed to be dominated by  $F\bar{F}$  in the 4.17 GeV energy region and by  $F\bar{F}^*$  in the 4.42 GeV region. The expected shape of the contribution to the  $M(\gamma\gamma)$  spectrum from this source has been calculated by Monte Carlo using as an input the statistical isospin model for F decay by Quigg and Rosner [3]. In the calculation a 16% semileptonic decay ratio, 38% hadronic decays with an  $\eta$  and 9% with an  $\eta'$  in the various final states were assumed whose frequency is also specified by the model. At 4.17 GeV and 4.42 GeV where this method has been applied, the fit of the 2 distributions to the observed  $M(\gamma\gamma)$  spectrum gives answers consistent with those of method I. The dashed-dotted curves in fig. 1 describe the fitted sum of the two contributions.

In order to determine an  $\eta$  cross section one has to know the  $\eta$  detection-efficiency or acceptance. Due to the event selection criteria applied in the analysis the  $\eta$  acceptance does not only depend on the geometry

of the apparatus and the efficiency of its components, but also on the details of the production mechanism. Two models for  $\eta$  production were tried. Model 1 is the statistical isospin model already mentioned, model 2 is a phase space model assuming that on average 4.2 charged particles and 2.8  $\pi^0$ 's are produced together with an  $\eta$ . At 4.17 GeV model 1 gives an acceptance of 4.2% (showing slight variations with energy) whereas model 2 yields an acceptance of 3.5%. A 30% systematic error in the  $\eta$  cross section will be assumed due to the uncertainty in the acceptance values. For the  $\pi^0$  acceptance there is a larger discrepancy between the answers obtained from both models: model 1 gave a value of 0.33%, model 2 a value of 0.72%.

As a reliability check of the analysis method and the acceptance calculation the total  $\pi^0$  inclusive cross section was calculated from the number of observed  $\pi^0$ 's determined by analysis method I using the acceptance values from production model 1. At all energies those cross sections were consistent within 50% with  $(\sigma(\pi^+) + \sigma(\pi^-))/2$  as measured by the DASP detector [4].

Fig. 2 shows the total inclusive  $\eta$  cross section  $\sigma(\eta)$ , as a function of the c.m. energy, calculated using method I (solid lines), and using method II at 4.17 and 4.42 GeV (dashed lines). The acceptance values of model 1 have been used. It can be seen that while no  $\eta$  signal is seen at 4.03 GeV, a significant  $\eta$  production is seen between 4.10 and 4.70 GeV. Note that  $\eta$  production below 4.10 GeV is less than 0.5 nb. This is

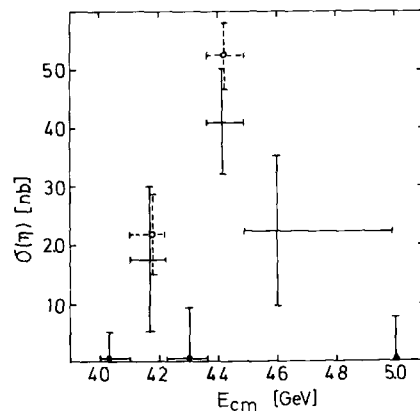


Fig. 2  $\eta$  inclusive cross section as a function of the c.m. energy, calculated according to method I (solid lines) and to method II (dashed lines).

much smaller than the pion or kaon production cross sections [4]. The following upper limit can be deduced for the D branching ratio into  $\eta$ 's, using the D cross section given in ref. [5] B.R. ( $D \rightarrow \eta + \text{anything}$ )  $< 2\%$ . Using their D cross section at 4.42 GeV, it would imply that  $\sigma(\eta, \text{ from D decay}) \leq 0.4 \text{ nb}$ , which is more than a factor 10 smaller than  $\sigma(\eta)$  at 4.42 GeV, implying that  $\eta$ 's at 4.42 GeV are produced by a different source. Using  $\sigma(\eta)$  at 4.42 GeV, and assuming that all of the 4.42 GeV resonance structure is due to F production, the following lower limit can be obtained. B.R. ( $F \rightarrow \eta X$ )  $\geq 34\%$ .

Fig. 3 shows the  $M(\gamma\gamma)$  mass distribution at 4.42 GeV for events having an electron in the DASP inner detector. The contamination due to hadrons simulating an electromagnetic shower has been estimated by looking at the process  $e^+e^- \rightarrow J/\psi \rightarrow \rho\pi \rightarrow \pi^+\pi^-\pi^0$ , and it was found to be  $1.2 \pm 0.5\%$  per charged track. The contamination due to photons converting in the beam pipe and Dalitz  $\pi^0$  decay was estimated to be less than 2.5% of the events. Folding those numbers

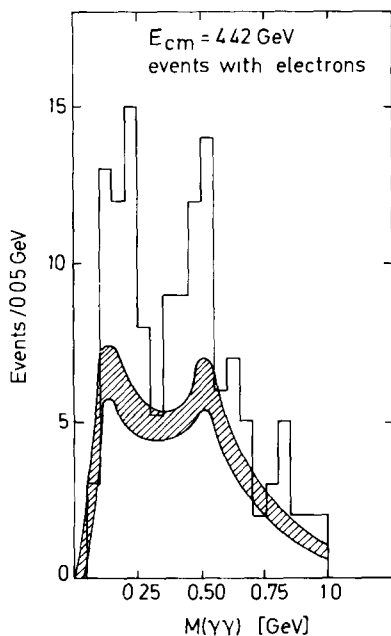


Fig. 3.  $M(\gamma\gamma)$  mass distribution at  $E_{c.m.} = 4.42 \text{ GeV}$ , for events having an electron in the DASP inner detector. The shaded band corresponds to a  $\pm 1\sigma$  uncertainty in the expected background from hadrons simulating an electron and photons converting in the beam pipe.

with the events that contributed to the  $M(\gamma\gamma)$  mass distribution in fig. 1, gives rise to the background distribution given in fig. 3 as a  $\pm 1\sigma$  band. Clear  $\eta$  and  $\pi^0$  peaks can be seen above this background, indicating that both are the decay products of weakly decaying states. While the  $\pi^0$ 's have their source in  $\tau$ , D and F production, the  $\eta$  signal cannot be due to the first two sources due to the lack of  $\eta$  signal at 4.03 GeV. Therefore the weakly decaying F meson becomes the most natural source of  $\eta$  production in this energy region.

In a previous publication [1] it was found that  $\eta$ 's are produced at the 4.42 GeV region in conjunction with a low energy photon ( $E_\gamma < 140 \text{ MeV}$ ), indicating that the dominant F production mechanism in this region occurs via the  $FF^*$  and/or  $F^*F^*$  channels. Fig. 4 shows the  $M(\gamma\gamma)$  distribution for events having a photon of less than 140 MeV/c momentum at c.m. energies below, in the 4.42 GeV region, and above it. While the first and last distributions do not show any strong  $\eta$  signal, the 4.42 GeV data show a clear  $\eta$  peak. Moreover, this signal lies on a smaller background than the one in fig. 1 for the same c.m. energy. This correlation of the  $\eta$  signal with events having a low energy photon is shown more clearly in fig. 5, where the ratio of events having a low energy photon to those that do not have, is shown as a function of  $M(\gamma\gamma)$ . A  $3.6\sigma$  peak at the  $\eta$  mass is seen, indicating that  $\eta$ 's at the 4.42 GeV region are produced in conjunction with a low energy photon, confirming the previous observa-

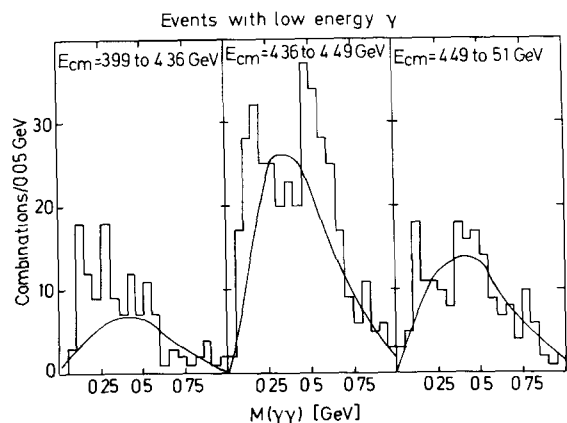


Fig. 4.  $M(\gamma\gamma)$  mass distribution for events having a low energy photon ( $E_\gamma < 140 \text{ MeV}$ ), below, at and above the 4.42 GeV  $E_{c.m.}$  region. The solid lines are estimates of uncorrelated photon background, normalized for  $M(\gamma\gamma) > 0.7 \text{ GeV}$ .

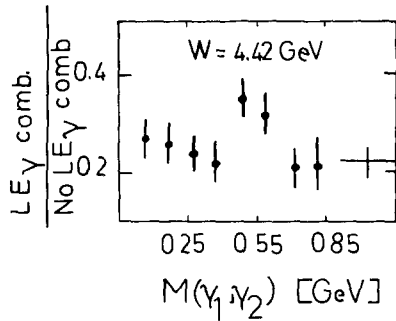
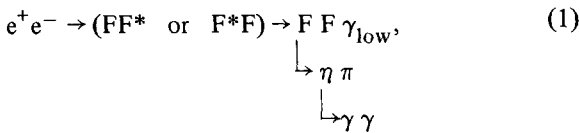


Fig. 5. Ratio of the number of combinations for events having a low energy photon to the number of combinations not having a low energy photon as a function of  $M(\gamma\gamma)$ , at  $E_{cm} = 4.42$  GeV

tion that  $FF^*$  or  $F^*F^*$  seem to be the dominant production mechanism.

Since the largest amount of  $\eta$  signal is observed at the 4.42 GeV region, the decay  $F \rightarrow \eta\pi \rightarrow \gamma\gamma\pi^\pm$  has been studied to determine the F meson mass. Candidates for the two body decay  $F \rightarrow \eta\pi$  were sought using the DASP outer spectrometers, which allow particle identification, and momentum measurement ( $\Delta(p)/p = 0.02 p$  (GeV/c)) of charged particles. To enter the fitting procedure a charged pion with momentum above 0.6 GeV/c was required, and at least two photons with energies above 0.1 GeV forming an  $M(\gamma\gamma)$  in the  $\eta$  region. One of the photons forming  $M(\gamma\gamma)$  had to be in the inner detector, while the second photon could be either in the inner detector or in the shower counter of the spectrometer arms. Finally there had to be at least one or more photon with an energy below 0.2 GeV ( $\gamma_{low}$ ). A total of 43 events satisfied these selection criteria at the 4.42 GeV region, and 79 events at all other energies. These events were fitted to the reactions:



These are 2C fits because of the mass constraint on

$M(\gamma\gamma)$  and the requirement that  $\pi\eta$  ( $\pi\eta\gamma_{low}$ ) and the missing vector must have the same mass  $m_F$  ( $m_{F^*}$ ) in the case of reaction (1) ((2)).

There were 15 events at the 4.42 GeV region and 11 events at all other energies that gave a fit to reaction (1) with  $\chi^2 < 8$ . By making the additional requirement  $|M_{fit}^{(\eta\pi)} - M_{meas}^{(\eta\pi)}| \leq 250$  MeV in order to cut on badly measured events, those numbers reduced further more to 12 and 10 events, respectively. Figs. 6a and 6c show the fitted  $\eta\pi$  mass versus the fitted recoil mass for the two regions. At 4.42 GeV a strong clustering is seen at  $M(\eta\pi) = 2.04$  GeV and  $M_{recoil} = 2.15$  GeV in fig. 6a while no such clustering is seen in fig. 6c for all other energies. All events in fig. 6c lie on a band given by the kinematics of the fit. Figs. 6b and 6d show the projections of figs. 6a and 6c along the  $M(\eta\pi)$  axis. A clear peak containing 6 events is seen at  $M(\eta\pi) = 2.04 \pm 0.01$  GeV for the 4.42 GeV data, while no such a peak is seen for all other energies; this implies that the background under the peak at 4.42 GeV is less than 0.2 event. The events at 4.42 GeV also give an acceptable fit to reaction (2) with a lower value for the F

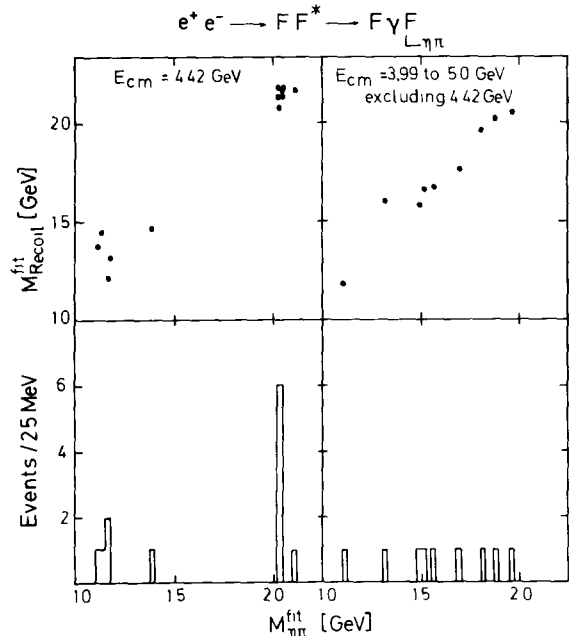


Fig. 6. Fitted  $\eta\pi$  mass versus fitted recoil mass, assuming  $e^+e^- \rightarrow FF^*$ , where  $F^* \rightarrow F\gamma$  and  $F \rightarrow \eta\pi$  at (a)  $E_{cm} = 4.42$  GeV and (c) at all other energies excluding 4.42 GeV. Histograms (b) and (d) are the projections of figs. (a) and (c), respectively, along the  $M(\eta\pi)$  axis.

Table 1

$E_{c.m}$ (GeV)	FF* fit			F F* fit	
	$M_F$ (GeV)	$M(F(\eta\pi), \gamma_{low})$ (GeV)	$M(F(\text{recoil}), \gamma_{low})$ (GeV)	$M_F$ (GeV)	$M_{F^*}$ (GeV)
4 400	$2.03 \pm 0.02$	$2.07 \pm 0.02$	$2.08 \pm 0.02$	$2.01 \pm 0.015$	$2.05 \pm 0.015$
4.400	$2.04 \pm 0.03$	$2.22 \pm 0.03$	$2.19 \pm 0.03$	$1.94 \pm 0.02$	$2.12 \pm 0.02$
4.400	$2.03 \pm 0.025$	$2.16 \pm 0.025$	$2.13 \pm 0.025$	$1.96 \pm 0.02$	$2.13 \pm 0.02$
4.380	$2.04 \pm 0.03$	$2.15 \pm 0.03$	$2.14 \pm 0.03$	$2.04 \pm 0.02$	$2.09 \pm 0.02$
4.416	$2.04 \pm 0.03$	$2.15 \pm 0.03$	$2.17 \pm 0.03$	$2.03 \pm 0.02$	$2.10 \pm 0.02$
4.422	$2.04 \pm 0.03$	$2.15 \pm 0.03$	$2.17 \pm 0.03$	$1.99 \pm 0.03$	$2.11 \pm 0.03$
	$\langle M_F \rangle = 2.04 \pm 0.01 \text{ GeV}$			$\langle M_F \rangle = 2.00 \pm 0.04 \text{ GeV}$	
	$\langle M_{F^*} \rangle = 2.15 \pm 0.04 \text{ GeV}$			$\langle M_{F^*} \rangle = 2.10 \pm 0.02 \text{ GeV}$	
	$M_F = 2.03 \pm 0.06 \text{ GeV}$				
	$M_{F^*} = 2.14 \pm 0.06 \text{ GeV}$				

mass ( $M(\eta\pi) = 2.00 \text{ GeV}$ ). The spread in the  $M(\eta\pi)$  distribution is slightly larger than in the case of hypothesis (1), as expected due to the ambiguity in the determination of the  $F^* \leftrightarrow \gamma_{low}$  relation. Table 1 presents the mass values for the two fits. Allowing for possible systematic uncertainties, the best estimate is  $m_F = 2.03 \pm 0.06 \text{ GeV}^{\dagger 2}$ .

The mass difference between  $F^*$  and  $F$  can be directly determined from the energy of the  $\gamma_{low}$  for the six events in the  $\eta\pi$  mass peak. The result is  $m_{F^*} - m_F = 0.11 \pm 0.046 \text{ GeV}$ . The cross section for those six events is found to be  $0.41 \pm 0.18 \text{ nb}$ , giving

$$\text{BR}(F \rightarrow \eta\pi) / \text{BR}(F \rightarrow \eta + \text{anything}) = 0.09 \pm 0.05 (\pm 30\% \text{ syst.}), \quad (3)$$

consistent with the assumption made in the Monte Carlo model (0.062) to compute the  $\eta$  acceptance.

Since a strong  $\eta$  signal is seen at the 4.17 GeV region, a search was made for events that would fit the process



<sup>†2</sup> Another group [6] has reported a preliminary observation of a peak in the  $K^+K^- \pi^\pm$  mass distribution at  $E_{c.m} = 4.16 \text{ GeV}$ . The mass value for this peak is  $2039 \pm 1.0 \text{ MeV}$ , consistent with the mass value for the  $\eta\pi$  decay mode given in ref. [1].

The selection criteria were the same as those imposed for reactions (1) and (2), except that no requirement was made on the presence of a  $\gamma_{low}$ . After imposing a  $\chi^2$  cut at 8, five events survived; only one event is above  $M = 1.95 \text{ GeV}$ . This event has a mass of  $2.03 \pm 0.02 \text{ GeV}$ , which is consistent with the  $F$  mass value found at the 4.42 GeV region.

**Conclusions.** Strong  $\eta$  production is observed at the 4.42 GeV resonance, while a threshold in  $\eta$  production is seen in the 4.17 GeV region. No  $\eta$  production is observed in the 4.03 GeV region where  $D$  production is the dominant production process. The  $\eta$  production is seen to be correlated with an electron, indicating that its main source is a weakly decaying particle, and most probably the  $F$  meson. Analysing events containing  $\eta$ ,  $\pi$  and a low energy photon in the final state, and fitting those events to either  $e^+e^- \rightarrow FF^*$  or  $F^*F^*$ , six events are found that give the same  $m_F$  value,  $m_F = 2.03 \pm 0.06 \text{ GeV}$  and  $m_{F^*} = 2.14 \pm 0.06 \text{ GeV}$ . From the energy distribution of the low energy photon, the  $F^* - F$  mass difference is found to be  $0.110 \pm 0.046 \text{ GeV}$ . The relative branching ratio of this decay mode was measured to be  $\text{B.R.}(F \rightarrow \eta\pi) / \text{B.R.}(F \rightarrow \eta + X) = 0.09 \pm 0.04 (\pm 30\% \text{ systematic})$ .

We would like to thank the engineers and technicians from DESY and the collaborating institutions who made this experiment possible by building, operating and maintaining DESY, DORIS, DASP and the

computer center. The non-DESY members of the collaboration thank the DESY directorate for their hospitality.

### *References*

- [1] R. Brandelik et al, Phys Lett. 70B (1977) 132.
- [2] R. Brandelik et al., Phys. Lett. 67B (1977) 243, 67B (1977) 358.
- [3] J.L. Rosner, Invited talk given at Orbis Scientiae - 1977, Coral Gables, Fla. C00-2220-120 (1977), C. Quigg and J. Rosner, FERMLAB-PUB-77/60-THY (1977).
- [4] R. Brandelik et al, to be published in Nucl Phys
- [5] I. Peruzzi and M. Piccolo, Contribution paper to Festschrift for C. Peyrou, LNF-78/12(P), March, 1978.
- [6] D. Luke, Invited talk given at the 1977 Meeting of the division of particles and fields of the A.P.S., Argonne, II, October 1977. SLAC-PUB-2086 (1978), A. Barbaro-Galtieri, private communication